Theoretical Studies of Oxidative Addition and Reductive Elimination: $H_2 + Pt(PH_3)_2 \rightarrow Pt(H)_2(PH_3)_2$

John J. Low and William A. Goddard III*

Contribution No. 6995 from the Arthur Amos Noyes Laboratory of Chemical Physics, California Institute of Technology, Pasadena, California 91125. *Received March 5, 1984*

Abstract: Ab initio calculations (Hartree–Fock, generalized valence bond, and configuration interaction), utilizing relativistic core potentials, have been used to follow the oxidative addition of H_2 to $Pt(PH_3)_2$. We find an activation barrier of 2.3 kcal/mol and an exothermicity of 15.9 kcal/mol. From examination of the geometries and wave functions, we find that up to the transition state the H–H bond is still intact. The role of the Pt s^1d^9 and d^{10} states in oxidative addition is described, and the effects of including electronic correlation are discussed. The implications for reductive elimination of the dimethyl and hydridomethyl complexes are also discussed.

I. Introduction

Oxidative addition and reductive elimination are important steps in many organometallic reactions.[1] In particular, the oxidative addition of a hydrogen molecule to a PtL_2 complex (where L is a substituted phosphine) has been observed for a number of different ligands, L [e.g., $P(c\text{-}C_6H_{11})_3$, $P(i\text{-}Pr)_3$].[2,3] H_2PtL_2 complexes have been observed to undergo many types of reactions, including insertion,[4-6] e.g.,

$$trans\text{-}H_2Pt[P(c\text{-}C_6H_{11})_3]_2 + CS_2 \rightarrow trans\text{-}HPt(S_2CH)\{P(C_6H_{11})3]_2$$

dimer formation,[7,8] e.g.,

$$2cis\text{-}H_2Pt[(t\text{-}Bu)_2P(CH_2)_3P(t\text{-}Bu)_2] \rightarrow 2H_2 + [Pt(t\text{-}Bu)_2P(CH_2)_3P(t\text{-}Bu)_2]_2$$

metallation,[9] e.g.,

$$2trans\text{-}H_2Pt[P(t\text{-}Bu)_3]_2 \rightarrow H_2 + [((t\text{-}Bu)_2PC(CH_3)_2\overline{CH_2})PtH]_2$$

and oxidative addition followed by reductive elimination of H_2,[2,3,10-12] e.g.,

$$trans\text{-}H_2Pt[P(c\text{-}C_6H_{11})_3]_2 + SiH_4 \rightarrow HPt(SiH_3)[P(c\text{-}C_6H_{11})_3]_2 + H_2$$

Such species have also been proposed as intermediates in the catalysis of the water–gas shift reaction[13] and of alkene hydrogenation.[7]

As a first step in gaining a better understanding of the formation of covalent bonds through reductive elimination and the scission of bonds via oxidative addition, we have examined the process

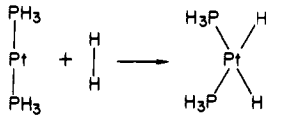

(1)

Of particular interest in analyzing these results will be to explain why (i) the addition of hydrogen to PtL_2 occurs at room temperature, but reductive elimination is quite slow;[2,3,14] (ii) the reductive elimination of methane from $(H)(CH_3)Pt(L)_2$ proceeds at room temperature;[15] but (iii) Pt(II) diakyl complexes tend be stable with respect to forming carbon–carbon bonds through reductive elimination. Thus, diakyl complexes will disproportionate through β-hydride elimination

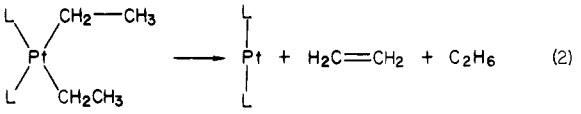

(2)

rather than reductively eliminate when they thermally decompose.[16-20] Only for Pt(II) diaryl complexes, where β-elimination is impossible, have carbon–carbon bonds been formed through reductive elimination at high temperatures.[21] On the other hand, (iv) Pd(II) dimethyl complexes are quite unstable with respect to reductive elimination to yield C–C coupling.[22]

In this paper we develop a relatively simple model of reaction 1 by examining the energetics, geometries, and wave functions along the reaction coordinate. These results indicate that oxidative addition of H_2 to PtL_2 depends crucially on the relative positions of the $5d^{10}$ and $6s^15d^9$ states of the platinum atom. The resulting energetics explain the observed differences regarding oxidative

(1) Collman, J. P.; Hegedus, L. S. "Principles and Applications of Organotransition Metal Chemistry"; University Science Books: Mill Valley, CA, 1980; Chapter 4.
(2) Yoshida, T.; Otsuka, S. *J. Am. Chem. Soc.* **1977**, *99*, 2134–2140.
(3) Fornies, J.; Green, M.; Spencer, J. L.; Stone, F. G. A. *J. Chem. Soc., Dalton Trans.* **1977**, 1006–1009.
(4) Albinati, A.; Musco, A.; Carturan, G.; Strukel, G. *Inorg. Chim. Acta* **1976**, *18*, 219–223.
(5) Immirzi, A.; Musco, A. *Inorg. Chim. Acta* **1977**, *22*, L35–L36.
(6) Clark, H. C.; Goel, A. B.; Wong, C. S. *J. Organomet. Chem.* **1978**, *152*, C45–C47.
(7) Yoshida, T.; Yamagata, T.; Tulip, T. H.; Ibers, J. A.; Otsuka, S. *J. Am. Chem. Soc.* **1978**, *100*, 2063–2073.
(8) Tulip, T. H.; Yamagata, T.; Yoshida, T.; Wilson, R. D.; Ibers, J. A.; Otsuka, S. *Inorg. Chem.* **1979**, *18*, 2239–2250.
(9) Clark, H. C.; Goel, A. B.; Ogini, W. O. *J. Organomet. Chem.* **1978**, *157*, C16–C18.
(10) Ebsworth, E. A. V.; Maranian, V. M.; Reed, F. J. S.; Gould, R. O. *J. Chem. Soc., Dalton Trans.* **1978**, 1167–1170.
(11) Clark, H. C.; Goel, A. B.; Billard, C. *J. Organomet. Chem.* **1979**, *182*, 431–440.
(12) Paonessa, R. S.; Trogler, W. C. *Organometallics* **1982**, *1*, 768–770.
(13) Yoshida, T.; Ueda, Y. Otsuka, S. *J. Am. Chem. Soc.* **1978**, *100*, 3941–3942.
(14) Paonessa, R. S.; Trogler, W. C. *J. Am. Chem. Soc.* **1982**, *104*, 1138–1140.
(15) Abis, L.; Ayusman, S; Halpern, J. *J. Am. Chem. Soc.* **1978**, *100*, 2915–2916.
(16) Whitesides, G. M.; Gaasch, J. F.; Stedronsky, E. R. *J. Am. Chem. Soc.* **1972**, *94*, 5258–5270.
(17) Nuzzo, R. G.; McCarthy, T. J.; Whitesides, G. M. *J. Am. Chem. Soc.* **1981**, *103*, 3404–3410.
(18) McCarthy, T. J.; Nuzzo, R. G.; Whitesides, G. M. *J. Am. Chem. Soc.* **1981**, *103*, 1676–1678.
(19) McCarthy, T. J.; Nuzzo, R. G.; Whitesides, G. M.; *J. Am. Chem. Soc.* **1981**, *103*, 3396–3403.
(20) Komiya, S.; Yoshiyuki, M.; Yamamoto, A.; Yamamoto, T. *Organometallics* **1982**, *1*, 1528–1536.
(21) Braterman, P. S.; Cross, R. J.; Young, G. B. *J. Chem. Soc., Dalton Trans.* **1976**, 1310.
(22) Gillie, A.; Stille, J. K. *J. Am. Chem. Soc.* **1980**, *102*, 4933–4941.

0002-7863/84/1506-6928$01.50/0

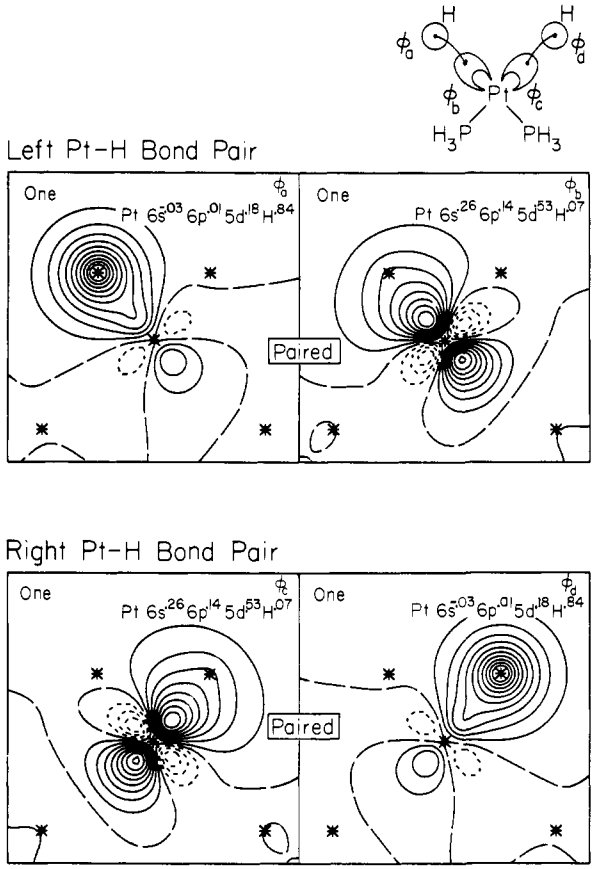

Figure 1. GVB orbitals for the Pt–H bonds of $H_2Pt(PH_3)_2$ at equilibrium. Hybridization for each singly occupied GVB orbital is shown on each plot. Each contour represents a change of 0.05 in amplitude. Solid lines represent positive amplitude. Dashed lines represent nodes. Dotted lines represent negative amplitude. Asterisks represent the position of atoms.

addition/reductive elimination in Pt and Pd complexes.

II. Summary of Results

The details of the calculations are described in section IV. Here we will emphasize the main lessons from the theoretical studies.

In the ground state of the reactants,

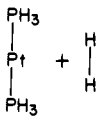

I

the lone pairs of the phosphines make strong Lewis base bonds to the Pt atom, stabilizing the (d^{10}) configuration and leading to a linear complex. The oxidative addition product is square-planar,

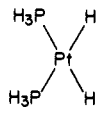

II

with an HPtH angle of 79.4° and a PPtP angle of 99.9°. Despite the terminology "oxidative addition", we find that there is essentially no charge transfer from the Pt to the H's. Instead, we find that the Pt in II corresponds to a $(6s)^1(5d)^9$ configuration of Pt, allowing the formation of two covalent bonds to the H atoms. The generalized valence bond (GVB) orbitals for these bond pairs are shown in Figure 1 where each bond involves one electron in an H1s-like orbital and one electron in a 6s–5d hybrid (60% d) pointing at the H.

The net exothermicity of reaction 1 is calculated to be 16 kcal/mol, so that one can consider the two Pt–H bonds of II to be worth 60 kcal/mol each. [If the geometry of the $Pt(PH_3)_2$ fragment were kept fixed, then the average Pt–H bond energy would be 72 kcal/mol.] The next question is how do the orbitals change as the system goes from I to II? This process is orbital symmetry allowed[23] and indeed we find in Figure 2 that the reaction has only a 2.3-kcal/mol barrier. In examining the potential curve in Figure 2, three distinct phases in the process of oxidative addition are discerned.

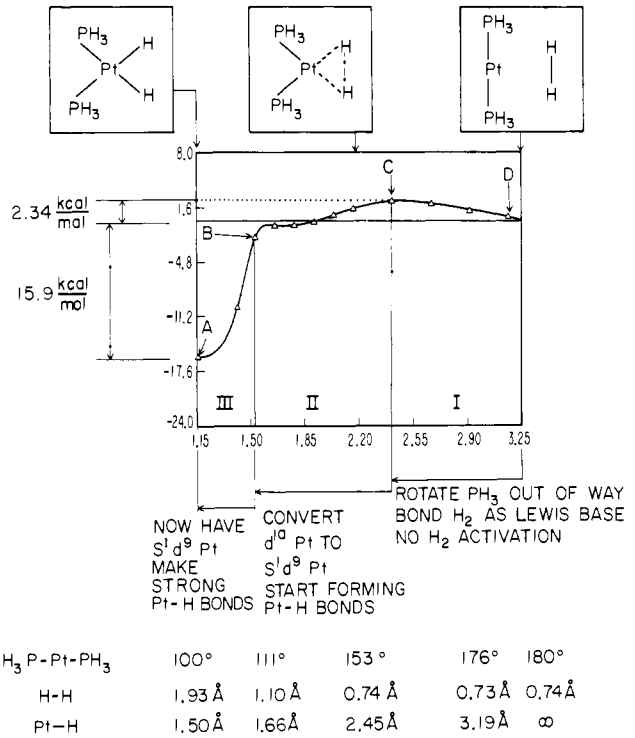

H_3P-Pt-PH_3	100°	111°	153°	176°	180°
H-H	1.93 Å	1.10 Å	0.74 Å	0.73 Å	0.74 Å
Pt–H	1.50 Å	1.66 Å	2.45 Å	3.19 Å	∞

Figure 2. Potential energy curve along the reaction coordinate.

(i) Lewis Base/Lewis Acid Bonding of H_2 to $Pt(PH_3)_2$ (D → C in Figure 2). Since the platinum atom is in a d^{10} state, the Pt 6s orbital is empty and can serve as an electron acceptor. As the hydrogen molecule approaches the diphosphine complex, the H_2 electrons utilize the Pt 6s orbital, making a Lewis acid/Lewis base bond. As this occurs, the phosphine ligands bend back (a) to lower steric interactions between the hydrogen molecule and the phosphine ligands and (b) to increase the overlap between the Pt 6s orbital and the H–H bonding orbital. The overlap between the Pt 6s and H–H bonding orbitals increases because the Pt 6s orbital polarizes away from the phosphines (hybridizes with the 6p orbital) to get orthogonal to the phosphine lone-pair orbitals. By the transition state, the P–Pt–P bond angle has decreased from 180° to 153°, but the H–H bond length remains essentially constant (changing by only 0.003 Å). The overall energy increase is 2.3 kcal/mol, whereas to bend the P–Pt–P angle the same amount in the diphosphine complex would cost 9 kcal/mol. Therefore we can consider the H_2–Pt Lewis base/Lewis acid interaction to be worth 7 kcal/mol at the transition state.

(ii) Electronic Promotion of the Platinum Atom (C → B in Figure 2). Once the H_2 molecule has passed the transition state (point B in Figure 2), the platinum atom begins to build in some d^9s^1 character. As the phosphines bend back from 153° to 113°, this becomes more favorable because the splitting between the d^{10} ($^1A_1$) ground state and the lowest s^1d^9 state ($^3B_2$) decreases as the P–Pt–P angle decreases. Thus, as the P–Pt–P angle decreases from 180° to 140° and then to 90°, this splitting decreases from 107 kcal/mol, to 63 kcal/mol, and then to 20 kcal/mol. The mixing of the d^9s^1 and the d^{10} states occurs mainly through the delocalization of the H_2 electrons into the Pt 6s orbital and the back-donation of the Pt $6d_{yz}$ electrons into the H–H antibonding

(23) Tatsumi, K.; Hoffmann, R.; Yamamoto, A.; Stille, J. K. *Bull. Chem. Soc. Jpn.* **1981**, *54*, 1857.

orbital. As these electronic changes occur, the H–H bond lengthens from 0.74 to 0.87 Å.

(iii) Covalent Bonding (B → A in Figure 2). By point B in Figure 2, the platinum atom is in the d^9s^1 state, allowing it to form two covalent Pt–H bonds. As the Pt–H bonds decrease from 1.72 Å to their equilibrium bond lengths (1.50 Å), the energy decreases rapidly. In this region the P–Pt–P bond angle changes from 113° to 100° and the H–H distance increases from 0.87 to 1.93 Å.

An important point from the calculations is that the final bonds are covalent; thus the *oxidative addition of* H_2 to Pt is *not oxidative*. Rather, the electronic state of the Pt is *promoted* from d^{10} to s^1d^9 because the d^{10} state cannot make covalent bonds, while the s^1d^9 state can make two covalent bonds. Therefore one might denote these states as Pt^0 and Pt^{II}, respectively, where the *superscript indicates not oxidation state but rather maximum covalency* (maximum number of covalent bonds). Substantiation of this idea that H_2 addition is not oxidative is given by the observed promotion of H_2 addition to Ir(I) complexes by *electron-withdrawing* substituents (opposite of the expected trend if one has assumed significant charge transfer to the hydrogens).[24]

A second point of the calculations is that a low barrier for the H_2 oxidation requires that the adduct (H_2) must be a sufficiently good Lewis base that it can activate the Pt by pushing back the phosphine ligands while forming a Lewis acid–base bond. The activation of the Pt corresponds to the stabilization of the s^1d^9 (Pt^{II}) state that can form the covalent bonds.

Implications for other systems are as follows. Preliminary calculations for

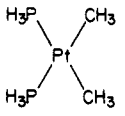

III

indicate an average Pt–C bond energy of $\bar{D}_{PtC}$ = 36 kcal/mol, whereas the work presented here leads to $\bar{D}_{PtH}$ = 60 kcal/mol. Extrapolating the same bond energies to $H(CH_3)Pt(PH_3)_2$ gives the following energetics:

$$Pt(PH_3)_2 + H_3C\text{–}CH_3 \rightarrow (PH_3)_2Pt(CH_3)_2 \quad \Delta E = +19 \text{ kcal/mol}$$

$$Pt(PH_3)_2 + H\text{–}CH_3 \rightarrow (PH_3)_2Pt(H)(CH_3) \quad \Delta E = +9 \text{ kcal/mol}$$

$$Pt(PH_3)_2 + H_2 \rightarrow (PH_3)_2PtH_2 \quad \Delta E = -16 \text{ kcal/mol}$$

The above energetics can be used to explain the relative energetics of hydridomethylplatinum(II) and of dihydride complexes. The platinum dihydrides are stable under 0.5 atm of hydrogen at room temperature and decompose slowly under vacuum.[14] The only known *cis*-hydridomethylplatinum(II) complex decomposes quickly at room temperature.[15] Since the Pt(II) dimethyl complex has been calculated to have a larger driving force for reductive elimination, and it is known experimentally that these complexes are more stable than the hydridomethylplatinum(II) complex, there must be a larger barrier to reductively eliminate ethane than to reductively eliminate methane. This is plausible since the directional character of the Pt–C bond requires that the methyl groups must rotate away from the Pt in order to overlap each other in forming the C–C bond. In contrast, for H_2 the s orbital used in the Pt–H bond can also be used in the H–H bond. Thus, for reductive elimination of ethane directly from $L_2Pt(CH_3)_2$, it is plausible that a barrier exists even if the process is exothermic. (Preliminary calculations on this process for a Pd complex confirm these expectations.[25])

On the other hand, in the hydridomethyl complex, the hydrogen orbital can overlap both the carbon sp^3 orbital and a Pt sd hybrid orbital as methane reductively eliminates. This should lead to an activation barrier for reductive elimination of methane from hydridomethylplatinum(II) complexes that is intermediate between those for breaking H–H and forming C–C bonds, in agreement with the observed reactivities of hydridomethyl complexes.[15]

We find that oxidative addition of H_2 to $Pt(PH_3)_2$ proceeds with a small activation barrier (2.3 kcal/mol) and the overall reaction is sufficiently exothermic that the products should be stable with respect to reductive elimination. This is in agreement with the results of Paonessa and Trogler.[14] They have prepared the dihydrides of the sterically unhindered $Pt(PMe_3)_2$ and $Pt(PEt_3)_2$ and found these complexes to be stable under 0.5 atm of H_2 and to decompose slowly under vacuum. The singular difference between Pd and Pt is that the Pd atom prefers the d^{10} configuration by 22 kcal/mol,[26] while Pt prefers the d^9s^1 configuration by 11.0 kcal/mol.[26] Thus Pd has a total bias of about 33 kcal/mol in favor of the d^{10} configuration. Since the reductive eliminations considered here involve mostly changing from s^1d^9 to d^{10}, this means that the increased splitting should make the Pd(II) complexes considerably (about 34 kcal/mol) less stable than their Pt counterparts. This is in agreement with observed reductive elimination of ethane from $Pd(CH_3)_2L_2$ complexes[22] (where L = PPh_3, PPh_2CH_3; L_2 = $PPh_2PCH_2CH_2PPh_2$) and the fact that hydrogen will not oxidatively add to a Pd diphosphine complex but does add for the corresponding platinum complex.[2]

Table I. Pt Atom State Splittings (in kcal/mol)

state	expt[c]	HF	GVB-(5/10)[a]	RCI-(5/10)[a]	GVBCI-(5/10)[a]
$^3D(s^1d^9)$[b]	0.0	0.0	0.0	0.0	0.0
$^1S(d^{10})$	11.0	31.4	27.0	12.3	12.2
$^3F(s^2d^8)$	14.7	8.4	11.2	18.5	14.2

[a] See Calculational Details section. [b] The total energies of the ^3D state are −27.506 19 hartrees at the HF level, −27.519 33 hartrees at the GVB–PP level, and −27.551 29 hartrees at the RCI(5/10) level (using the relativistic effective core potential of ref 37). [c] The energies in this column are actually the average of experimentally observed j states derived from each Russell–Sanders term.

III. Results

A. Platinum Atom. The changes occurring during oxidative addition are partly determined by the electronic structure of the Pt atom. As with Ni and Pd, the platinum atom has three low-lying states, $^3D(s^1d^9)$, $^1S(d^{10})$, and $^3F(s^2d^8)$. We find that the Pt complexes tend to have the character of one or another of these atomic states and that the chemistry is dominated by this atomic character. In Table I, we summarize the relative energies of these states for various levels of calculations and experimental results.[27]

Clearly, Hartree–Fock (HF) calculations are strongly biased *against* the d^{10} state. In the jargon of theorists, electron correlation is far more important if the two electrons are in a 5d orbital than if the electrons are in different orbitals (5d or 6s). A simple way to account for the major electron correlation errors implicit in the HF or molecular orbital (MO) description is the use of the GVB wave function, which allows each electron to have a differently shaped orbital and allows the orbitals for singlet-coupled electrons to overlap. Thus, in GVB each doubly occupied valence orbital of the HF wave function is described by a *pair* of overlapping GVB orbitals. For an atom with a doubly occupied d orbital in the HF wave function, the GVB wave function converges to one tight d orbital (near the nucleus) and one diffuse d orbital (farther from the nucleus). We have chosen to describe the doubly occupied s orbital of the ^3F state by tight and diffuse s orbitals in order to be consistent with the correlation included in the GVB pairs describing d electrons.[28]

(24) Crabtree, R. *Acc. Chem. Res.* **1979**, *12*, 331–388.
(25) Low, J. J.; Goddard, W. A., III *J. Am. Chem. Soc.*, submitted for publication.
(26) Moore, C. E. "Atomic Energy Levels"; National Bureau of Standards: Washington, DC, 1971; Vol. III (averaged over j states to cancel out spin–orbit coupling).
(27) Herzberg, G. "Molecular Spectra and Molecular Structure, Part III. Electronic Spectra and Electronic Structure of Polyatomic Molecules"; D. Van Nostrand Co., Inc.: Princeton, NJ, 1966.

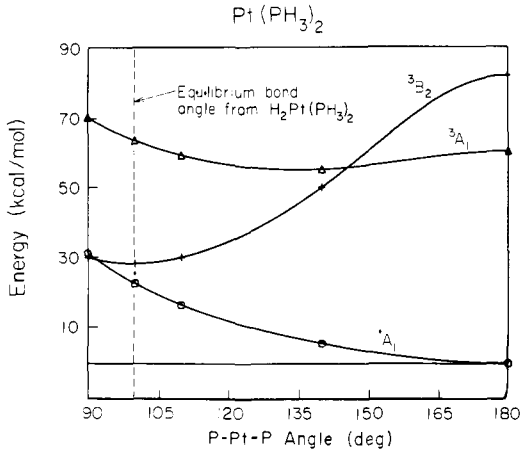

Figure 3. Potential energy curves for the low-lying states of $Pt(PH_3)_2$ as a function of P–Pt–P angle.

In many systems, electron correlation plays an important chemical role only for certain orbitals. In the platinum atom most of the electronic correlation important for state splittings occurs in the Pt 5d and 6s orbitals. Thus, if all ten d electrons in the Pt $^1S(d^{10})$ state are correlated in the GVB wave function, we denote this wave function as GVB(5/10) [here the 5 is the number of singlet-coupled electron pairs, while the 10 is the number of orbitals used to describe the five pairs]. If only one pair of electrons were to be correlated (i.e., for the bonding pair of electrons in Pt–H), we would use a GVB(1/2) wave function.

When there is more than one pair to correlate, there are additional options in describing the wave function. The simplest description is for each pair to have singlet spin coupling as a simple valence bond (VB) wave function. This is denoted as GVB–PP and is the usual form in which the orbitals are calculated. However, for a system with five pairs of electrons (ten VB orbitals), there are 42 VB structures or spin couplings that should all be included in calculating the final wave function. In addition, there are *inter*pair correlation effects, wherein if the two electrons in the d_{xy} orbitals are at some instant closer to the nucleus, the two electrons in the d_{yz} orbital will at that instant tend to be farther from the nucleus. These spin coupling and interpair correlation effects are included by carrying out a configuration interaction (CI) calculation in which the two electrons in each pair of orbitals are simultaneously allowed all possible occupations of those two orbitals, leading to what is termed a GVB–RCI wave function. Thus, for a GVB–PP(5/10) wave function, there are $3^5 = 243$ configurations in the GVB–RCI wave function.

The most complete wave function that can be described with just the GVB orbitals is to carry out a full CI with use of all possible occupations of these orbitals. This is termed GVB–CI, and for a GVB–PP(5/10) wave function, this leads to 8953 configurations. Since the GVB–RCI and GVB–CI are based on GVB orbitals, we can interpret these CI wave functions in terms of simple VB concepts. As is evident from the results in Table I, the GVB–RCI wave function gives results that are as consistent as the GVB–CI results but with significantly fewer configurations. For the purposes of this paper, the GVB–RCI provides the best combination of accuracy and simplicity.

B. $Pt(PH_3)_2$. When two phosphines are added to a platinum atom, the major effect is to raise the energy of the platinum 6s orbital relative to the Pt 5 d orbitals. This occurs because the phosphine lone pair makes a Lewis acid–base bond by overlapping with (donating into) the Pt 6s orbital. The net result is that the ground state of $Pt(PH_3)_2$ is a singlet ($^1A_1$) state derived from the $^1S(d^{10})$ state of the platinum atom. In this state, the phosphines minimize their steric replusions by increasing the P–Pt–P bond angle to 180°. The low-lying triplet states of $Pt(PH_3)_2$ are both derived from the $^3D(s^1d^9)$ state of the platinum atom. When two hydrogen atoms make bonds to $Pt(PH_3)_2$, we find that the Pt atom changes from d^{10} to s^1d^9 character in order to make covalent Pt–H bonds. In making these bonds, there is a major change in the P–Pt–P angle of PtL_2. In order to assess the role of this geometric change upon the energetics of the Pt d^{10} and s^1d^9 states, we show in Figure 3 the energies of the $Pt(PH_3)_2$ complex as a function of P–Pt–P bond angle. [The internal coordinates of the phosphine were frozen at the internal coordinates of free phosphine[27] (H–P–H angle = 93.3°, P–H bond distance = 1.420 Å). The Pt–P distance was chosen to be 2.268 Å.[30] The H–P–Pt angles were fixed (at 122.9°) so that the C_3 axis of the phosphine groups would pass through the platinum atom.]

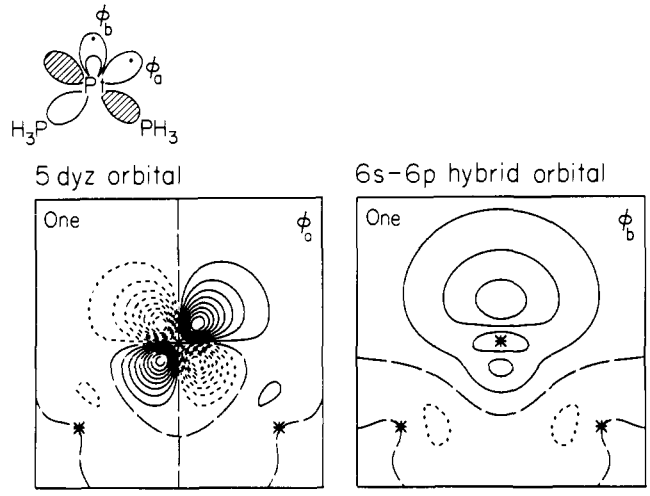

Figure 4. Open-shell orbitals for the $^3B_1$ state for bent (100°) $Pt(PH_3)_2$.

Table II. State Splittings for the d^{10} and d^9s^1 States of $Pt(PH_3)_2$

state	PH_3–Pt–PH_3 angle, deg	state splittings (kcal/mol) HF	GVB(5/10)	RCI(5/10)
$^1A_1$[a]	180.0	0.0	0.0	0.0
$^3B_2$	180.0	81.9	89.2	106.5
$^3A_1$	180.0	65.7	53.3	69.6
$^3B_2$	99.0[b]	28.5	35.2	51.5
$^1A_1$	99.0[b]	22.8	22.1	24.6
$^3A_1$	99.0[b]	72.9	58.0	75.3

[a] The total energies for the $^1A_1$ are −712.170 592 hartrees at the HF level, −712.199 127 hartrees at the GVB-PP(5/10) level, and −712.260 738 hartrees at the RCI(5/10) level. [b] 99.0° is the optimum bond angle for the $^3B_2$ state.

The lowest excited state of $Pt(PH_3)_2$ is the $^3B_2$ state with an s^1d^9 configuration. This state has a singly occupied $5d_{yz}$ orbital and a singly occupied 6s orbital. The phosphines would prefer to have their lone pairs overlap the singly occupied d_{yz} orbital as much as possible, which would imply a bond angel of 90° or 180°; however, the 90° geometry allows the 6s pair to hybridize away from the phosphines, stabilizing this geometry. Steric interactions of the phosphines cause the bond angle to open up slightly, leading to an optimum bond angle of 99.0° (HF). A plot of the singly occupied orbitals for the $^3B_2$ state is shown in Figure 4, where we note that the singly occupied 6s orbital has been polarized away from the phosphines. This occurs because the 6s orbital must be orthogonal to the phosphine lone pairs.

In Table II, we show the state splittings at various levels of calculation for several states.

The $^3A_1$ state has a singly occupied Pt d_{z^2} orbital and a singly occupied Pt p orbital (see Figure 5). In this case a bond angle of 180° is favored since the phosphines can both overlap the singly occupied d_{z^2} orbital while simultaneously minimizing their steric

(28) The best (lowest energy) two-orbital description of the 6s pair of electrons would be in terms of two sp hybrid orbitals, $\varphi_a = c_1\varphi_s + c_2\varphi_p$ and $\varphi_b = c_1\varphi_s - c_2\varphi_p$, as for Be, Mg, Zn, etc.[29]

(29) Goddard, W. A., III; Harding, L. B. *Annu. Rev. Phys. Chem.* **1978**, *29*, 363–396.
(30) Noell, J. O.; Hay, P. J. *J. Am. Chem. Soc.* **1982**, *104*, 4578–4584.

Table III. Summary of Results for Pt–H

	R, Å	D_e, kcal/mol	total energy,[e] hartrees	ω_e,[b] cm^{-1}	dipole moment,[c] Debye	Mulliken pop. on Pt	Mulliken pop. on H
HF	1.516	37.3	−28.065 612	2027	2.52	10.07	0.93
GVB–PP(1/2)	1.526	51.6	−28.088 370	1948	1.89	10.10	0.90
GVB–PP(5/10)	1.530	58.1	−28.098 619	1930	1.88	10.10	0.90
RCI(5/10)	1.544	48.9	−28.128 813	1914	1.86	10.11	0.89
GVB–CI(5/10)	1.549	52.8	−28.136 407	1909	1.90	10.10	0.90
DC–CI	1.51[d]	60.6					
experiment[a]	1.528	<79.3		2260			

[a] Huber, K. P.; Herzberg, G. "Molecular Spectra and Molecular Structure. IV. Constants of Diatomic Molecules"; Van Nostrand-Reinhold Co.: New York, 1979. [b] Frequencies were obtained from the curvature at R_e which was obtained from a cubic spline fit. [c] The positive sign implies Pt^+H^-. [d] This calculation was only carried out at this bond distance. [e] All total energies are reported for R = 1.51 Å.

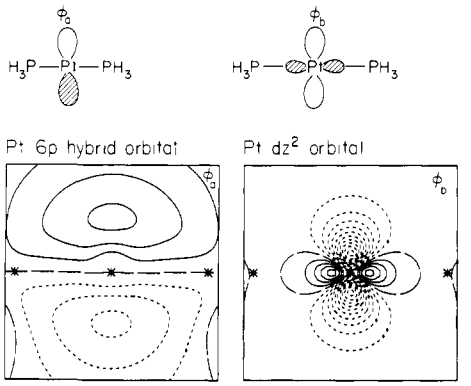

Figure 5. Open-shell orbitals for the $^3A_1$ state for linear $Pt(PH_3)$.

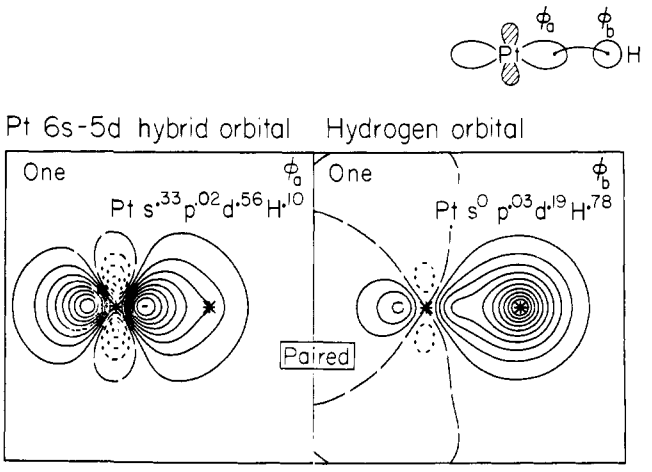

Figure 6. GVB orbitals for diatomic PtH.

interactions. However, in this geometry the s orbital cannot as easily polarize out of the way of the phosphine lone pairs, leading to a higher energy. In fact, for this state the Pt s electron has been promoted to the p orbital[31] (see Figure 5). The $^3B_2$ state is the best triplet because it allows both phosphines to overlap the singly occupied d orbital, while allowing the platinum s orbital to polarize out of the way of the phosphine lone pairs.

Comparisons between Pd and Pt complexes are useful because both atoms have low-lying d^9s^1 and d^{10} atomic states but yield different ground states. In palladium the atom has a d^{10} ground state (22.9 kcal/mol below the d^9s^1 state), while in platinum the d^9s^1 state is the ground state (11.0 kcal/mol below the d^{10} state). This should lead to d^{10}–s^1d^9 splittings for the Pd diphosphines that are 33.9 kcal/mol larger (disfavoring oxidative addition to Pd) and hence should result in much weaker Pd–H and Pd–C σ bonds for Pd diphosphine complexes than for the corresponding Pt complexes. Consistent with these expectations, hydrogen has not been observed to add to PdL_2 while it has for PtL_2 [e.g., L = $P(c\text{-}C_6H_{11})_3$, $P(i\text{-}Pr)_3$].[2] In addition, Gillie and Stille[22] have observed reductive elimination of ethane from Pd(II) dimethyl complexes, while Pt(II) dimethyl complexes are much more stable. These cases demonstrate how the d^{10}–s^1d^9 splittings for these ML_2 complexes affect the driving forces for reductive elimination and oxidative addition.

C. Pt–H. Calculations were performed on the platinum hydride diatomic molecule to determine how the energetics of the Pt–H bond are affected by the level of the calculations. These studies also help demonstrate the nature of the Pt–H bond. Five levels of calculation have been performed: HF, GVB(1/2), GVB(5/10), RCI(5/10), and GVB–CI(5/10). The results of these calculations are shown in Table III where we see that bond distance (R_e), bond energy (D_e), and vibrational frequency (ω_e) are fairly insensitive to the level of calculation once the Pt–H bond pair was correlated. Thus, description of the Pt–H bond at the GVB(1/2) level provides a quite adequate description of the bond and should be a suitable level for use in the Pt–H bonds in $H_2Pt(PH_3)_2$ and in reductive elimination from this complex.

Experimental characterization of PtH includes the bond length and vibrational frequency but only an upper bound for the bond energy. This compares well with the experimental geometry (1.5% long) but is 15% low for the vibrational frequencies. The best theoretical bond energy of 60.6 kcal/mol was obtained from a dissociation-consistent configuration interaction (DC–CI) calculation.[32] This calculation involves all single and double excitations from the active space defined by the Pt–H bond pair from a GVB–PP(1/2) calculation times all single excitations from the semiactive space defined by the remaining platinum valence electrons. This calculation was carried out at only a single point (1.51 Å), so a vibrational frequency is not reported for this level of calculation. This calculated bond energy is 20 kcal/mol smaller than the experimental upper bound of 80 kcal/mol.

The calculated Mulliken populations and dipole moments show that the PtH bond is essentially covalent. This is consistent with the small difference in Pauling electronegativities of Pt (2.2) and H (2.1).[33] However, detailed comparison of the dipole moment and Mulliken populations appears to give conflicting results. The dipole moment indicates a transfer of 0.26 e^- to the hydrogen atom, while the Mulliken populations indicate a transfer of 0.10 e^- from the H. This apparent conflict is partly due to the Pt part of the bond orbital being a Pt sd hybrid with some Pt p character so that is is polarized toward the hydrogen. This polarization contributes to the dipole moment but not to the Mulliken charge transfer. To obtain a qualitative measure of the polarization taking place, we have calculated the dipole moment of the platinum orbitals from a GVB(1/2) calculation on PtH. This calculation included the localized Pt GVB orbital from the Pt–H GVB bond pair and the other five Pt-like nonbonding sd orbitals (four doubly occupied and the singly occupied $d_{x^2-y^2}$ orbital), where in each case any hydrogen character was deleted (and the orbitals were renormalized). This calculation on the Pt atom yields a dipole moment of 1.08 D, over half the total dipole moment of Pt–H. Subtracting

(31) We have used C_{2v} symmetry to classify the states in this discussion. At a P–Pt–P angle of 180° the $Pt(PH_3)_2$ complex would actually have D_{3h} symmetry. The $^3A_1$ state would be one component of the $^3E'$ state.

(32) Bair, R. A.; Goddard, W. A., III *J. Chem. Phys.*, submitted for publication. Bair, R. A. Ph.D. Thesis, California Institute of Technology, 1981.

Table IV. Geometries along the Reaction Coordinates 1–13

	1	2	3	4	5	6	7	8	9	10	11	12	13
R_{Pt-H_2}[a]	1.166	1.417	1.542	1.667	1.792	1.917	2.042	2.167	2.417	2.667	2.917	3.167	∞
R_{Pt-P}	2.447	2.417	2.387	2.372	2.356	2.335	2.336	2.348	2.351	2.330	2.334	2.325	2.318
R_{H-H}	1.926	1.570	1.104	0.865	0.812	0.780	0.762	0.750	0.740	0.733	0.728	0.732	0.743
R_{Pt-H}	1.504	1.620	1.628	1.723	1.838	1.957	2.077	2.199	2.445	2.692	2.940	3.188	
R_{P-H_a}	1.525	1.522	1.519	1.524	1.525	1.525	1.526	1.529	1.530	1.525	1.518	1.526	1.527
R_{P-H_b}	1.529	1.526	1.526	1.526	1.525	1.526	1.525	1.527	1.526	1.525	1.522	1.527	1.527
θ_{P-Pt-P}[b]	99.9	102.5	108.1	113.5	122.3	127.2	133.8	137.4	152.9	167.2	170.1	175.2	180.0
θ_{H-Pt-H}	79.4	58.0	39.4	29.1	25.5	23.0	21.1	19.6	17.4	15.6	14.3	13.2	
$\theta_{H_a-P-H_b}$	96.6	96.8	95.9	95.3	95.0	95.2	94.9	94.8	95.1	95.6	94.3	95.7	96.2
$\theta_{H_b-P-H_c}$	95.5	95.5	95.5	94.9	94.7	94.8	95.2	95.0	95.5	95.7	95.8	95.8	96.2
θ_{H_a-P-Pt}	119.3	120.2	121.2	123.8	123.1	124.4	124.8	124.8	124.9	120.7	122.9	121.1	120.7
θ_{H_b-P-Pt}	121.4	120.9	121.0	120.4	121.1	120.2	120.0	120.2	119.7	121.4	121.3	121.1	120.7

[a] All R in Å. [b] All θ in deg.

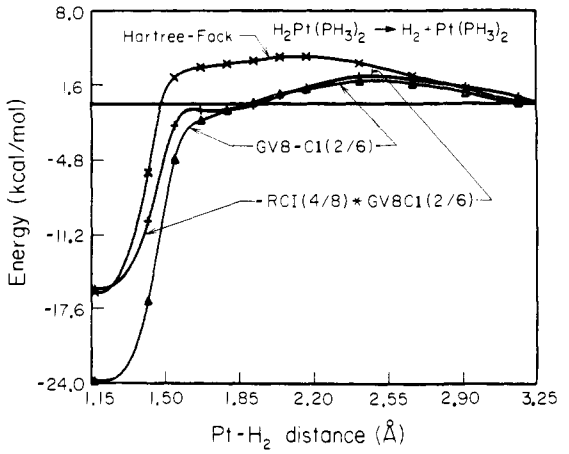

Figure 7. Plot of energy along the reaction coordinate for HF, GVB–CI(2/6), and RCI(4/8)*GVB–CI(2/6) wave functions.

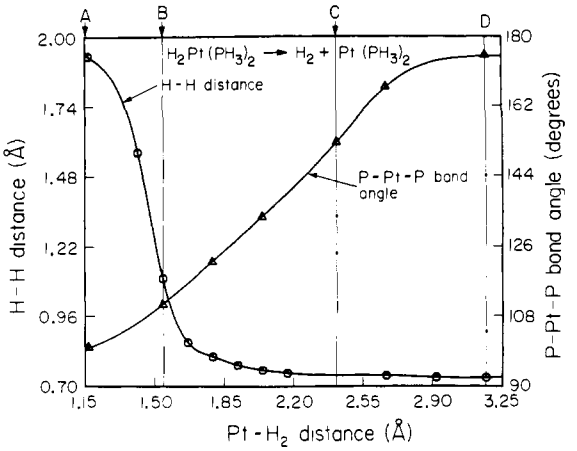

Figure 8. Changes in the P–Pt–P bond angle and H–H distance along the reaction coordinate.

this dipole moment due to Pt atom polarization from the total dipole moment leads to a residual molecular moment of 0.81 D, corresponding to a transfer of only 0.11 e^- to the hydrogen atom. Therefore, a large fraction of the dipole moment is due to polarization of the Pt valence orbitals. The remaining discrepancy of $Q_H = 1.11$ e^- from the dipole moment vs. $Q_H = 0.90$ e^- from the Mulliken populations represents a deficiency in the Mulliken analysis, namely, the equal partitioning of overlap terms tends to underestimate the population on H. Summarizing, the charge transfer in the Pt–H bond is small so that the Pt–H bond should be described as covalent.

The Mulliken populations for the GVB orbitals (see Figure 6) of the Pt–H bond show that the GVB orbital localized on the Pt atom is about 60% Pt d character and 40% Pt sp character. This hybridization of the Pt d_{z^2} orbital makes the density along the z axis larger than it would be for either a pure Pt 6s orbital or a pure Pt d_{z^2} orbital. This increases the overlap (and contragradience) between the platinum orbital and the hydrogen orbital.[34]

D. $H_2Pt(PH_3)_2$. The changes in the electronic structure that occur during oxidative addition can most easily be elucidated by following a reaction path from reactants to products. We used the distinguished coordinate method to find a good approximation to the reaction coordinate at various levels of calculation.[35] The distinguished coordinate method freezes one internal coordinate of the system to be studied while optimizing all the others for lowest energy. By repeating this procedure for a number of values for the frozen coordinate, one can generate a potential curve that is only a function of one variable and changes continuously from products to reactants. These optimizations were performed at the HF level with use of an analytic gradient technique.[36] HF

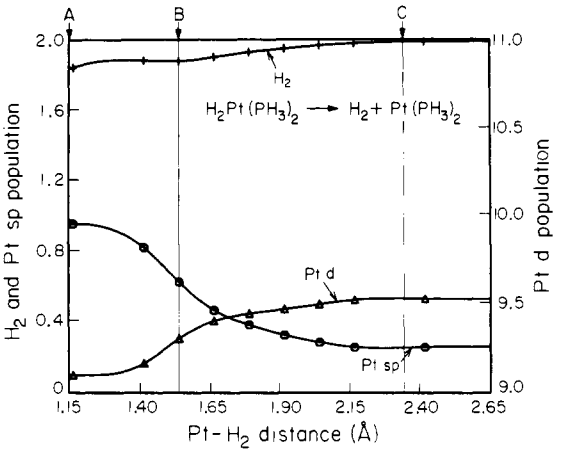

Figure 9. Muliken population along the reaction coordinate.

provides accurate equilibrium geometries for various platinum complexes[37] and leads to exothermicities and barrier heights similar to correlated wave functions.

The geometries resulting from the distinguished coordinate method are listed in Table IV. For more details on how these calculations were carried out, see section IV. The distinguished coordinate used in these calculations was the Pt–H_2 distance. The HF potential as a function of Pt–H_2 distance is shown in Figure 7.

As the Pt–H_2 distance was varied, only two other internal coordinates changed significantly. The P–Pt–P angle changed from 180° to 100° through the reaction path. The H–H distance increased a small amount as the hydrogen molecule approached the $Pt(PH_3)_2$ complex up to a Pt–H_2 distance of 2.0 Å. For Pt–H_2

(33) Pauling, L. "The Nature of the Chemical Bond", 3rd ed.; Cornell University Press: Ithaca, New York, 1960; pp 88–98.
(34) Steigerwald, M. L. Ph.D. Thesis, California Institute of Technology, 1983.
(35) Rothman, M. J.; Lohr, L. L. *Chem. Phys. Lett.* **1980**, *70*, 405.
(36) Low, J. J.; Goddard, W. A., III, manuscript in preparation.
(37) Noell, J. O.; Hay, P. J. *Inorg. Chem.* **1982**, *21*, 14–20.

distances less than 2.0 Å, the H–H distance increased rapidly from 0.76 to 1.926 Å. These geometry changes as a function of Pt–H_2 distance are shown in Figure 8.

E. Charge Populations. The Mulliken populations of the Pt d, Pt s and H_2 orbitals are plotted as a function of Pt–H_2 distance in Figure 9. This plot shows that the amount of Pt 6s character increases and the amount of Pt 5d character decreases as H_2 approaches the $Pt(PH_3)_2$ complex. At the dissociated limit, the Pt population has 9.51 d electrons and 0.38 s electrons. At equilibrium, the population has 9.10 d electrons and 0.96 s electrons. Although Mulliken populations are not truly quantitative measures for the character and locations of the electrons, as shown above for Pt–H, they can be used to provide qualitative ideas of how charge is distributed. At equilibrium, the Mulliken populations show that the platinum atom is in a d^9s^1 state. At the dissociated limit and at the transition state, the platinum atom is in a state that is mainly d^{10} and singlet.

In Noell's population analysis,[38] charges are assigned to atoms by partitioning space. All charge within the covalent radius of the Pt atom was assigned to this center. The space outside this sphere was partitioned into cones with 45° angles of rotation about each ligand. The charge in a particular cone was assigned to the ligand that was contained in the cone. The remaining charge outside the covalent radius of the platinum atom was assigned to the platinum atom. This partitioning resulted in a positively charged platinum atom (1.22 e^-), negatively charged hydrogen atoms (−0.29 e^-), and negatively charged PH_3 groups (−0.32 e^-). Noell feels that this is a more reasonable assignment because it is closer to the formal oxidation states of the platinum and hydrogen atoms. One problem with Noell's analysis is that a relatively large fraction of the platinum atom d basis (11%) and sp basis (37%) is outside the covalent radius of the platinum atom. When the platinum atom is in a s^1d^9 state, this would result in 1.36 e^- being assigned to the ligands! Clearly this is not a fair division of density.

Comparing the Pauling electronegativities[33] of platinum (2.2) and hydrogen (2.1), we see that the hydrogen atom should be slightly negatively charged. But such a small difference in the electronegativity should lead to a bond that is essentially covalent (less than 4% ionic by Pauling's formula).[33] The dipole moment of Pt–H indicates that the Pt–H bond is more polar than Pauling would predict, as discussed in section III. This is due largely to the polarization of the Pt valence electrons rather than to charge transfer. Although the Mulliken population leads to the wrong polarity (Pt^-H^+), it is paritcularly useful in determining the relative amounts of Pt s, p, and d character in a wave function. Qualitatively, the Mulliken populations indicate that there is not a large amount of charge transfer, and this is in agreement with the dipole moments.

F. Forms for the Wave Functions. In analyzing the character of bond orbitals, it is important to use wave functions that change smoothly as one goes from one extreme with a doubly occupied Pt d_{yz} orbital and H–H bond pair to the other extreme with Pt–H bonds. The simplest wave function providing a good description of the Pt–H bonds is the GVB(2/4) wave function. This wave function contains one GVB pair for each Pt–H bond, as shown in Figure 1. These orbitals involve combinations of the platinum $5d_{yz}$ and 6s orbitals and of the two hydrogen atomic orbitals. The best GVB orbitals at the dissociated limit are shown in Figure 10. These orbitals involve combinations of a tight Pt $5d_{yz}$ orbital, a diffuse $5d_{yz}$ orbital, and two hydrogen atomic orbitals. Thus the GVB(2/4) wave function is *not* consistent throughout the reaction path because different types of correlation are required to describe the electrons localized on the platinum atom at the different limits. At the dissociated limit, the pair of Pt electrons involved in the Pt–H bonds are both in d_{yz} orbitals and are correlated in–out. In other words, one electron is in close to the platinum atom while the other is farther away. After the two Pt–H bonds are formed, the bonding Pt electrons are both in sd hybrid orbitals.

A more consistent wave function for this reaction would be to allow the Pt pair of bonding electrons to use a tight d orbital, a diffuse d orbital, and a Pt s orbital. This would allow this pair of electrons to have both in–out correlation and the optimum d^9s^1 mixture throughout the reaction. In order that the two GVB pairs involved in the bonding be treated equivalently, we have permitted each of them to have three natural orbitals (rather than two). At the dissociated limit, this corresponds to a Pt pair, as was described above, and to an H_2 molecule described at the GVB(1/3) level (in–out plus left–right correlation).

In considering the effects of electron correlation on this reaction, we examined the HF, GVB–CI(2/6), and GVB–CI(2/6)*RCI-(4/8) wave functions. The GVB–CI(2/6) wave function includes electronic correlation terms differential in describing the Pt–H bonds. The GVB–CI(2/6)*RCI(4/8) wave function includes both the Pt–H bonding terms of the GVB–CI(2/6) level as well as the d–d correlations important in determining the d^9s^1–d^{10} splitting on the platinum atom. For more calculational details, see section IV.

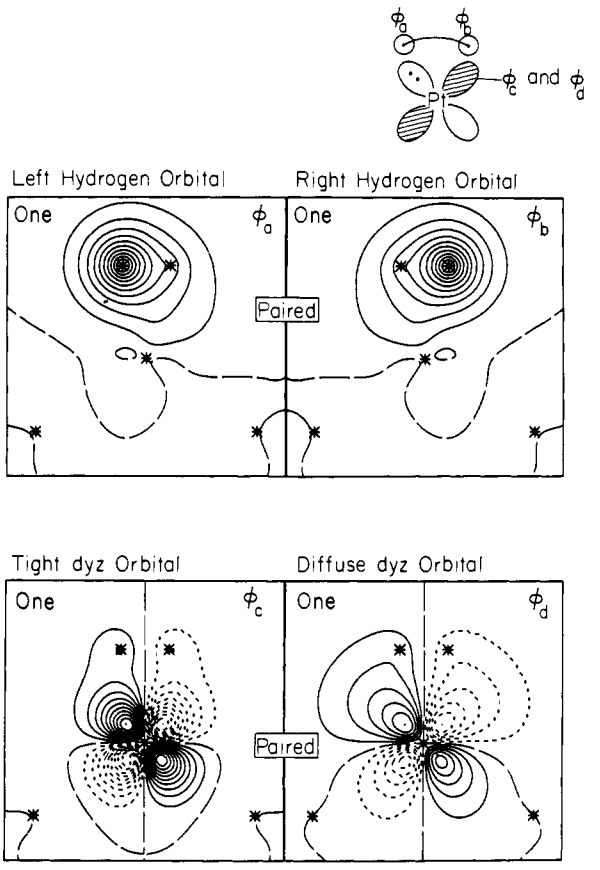

Figure 10. GVB orbitals for H_2 + $Pt(PH_3)_2$ near the transition state.

Table V. Energies along the Reaction Path

R_{Pt-H_2}, Å	HF, kcal/mol	GVB–CI(2/6), kcal/mol	GVB–CI(2/6)-*RCI(4/8), kcal/mol
1.166	−16.21	−23.79	−15.90
1.417	−5.92	−16.91	−10.09
1.542	2.26	−4.76	−1.86
1.667	3.12	−1.41	−0.56
1.792	3.42	−0.55	−0.51
1.917	3.69	0.13	−0.13
2.042	4.00	0.86	0.70
2.167	4.04	1.25	1.40
2.417	3.47	1.96	2.34
2.667	2.37	1.71	2.05
2.917	1.26	0.92	1.40
3.167	0.15	0.02	0.52
∞[a]	0.0	0.0	0.0

[a] The total energies at the dissociated limit (∞) are −713.330 533 hartrees at the HF level, −713.363 061 hartrees at the GVB–CI(2/6) level, and −713.449 931 hartrees at the GVB–CI(2/6)*RCI(4/8) level.

Table VI. Transition State as a Function of Electronic Correlation for $Pt(PH_3)_2 + H_2 \rightarrow H_2Pt(PH_3)_2$

level of electronic correlation	$Pt-H_2$ distance, Å	activation energy, kcal/mol	exothermicity, kcal/mol
HF	2.199	4.04	−16.21
GVB–CI(2/6)	2.417	1.96	−23.79
RCI(4/8)*GVB–CI(2/6)	2.417	2.34	−15.90

Table VII. Comparison of the HF Activation Barrier for $Pt(PH_3)_2 + H_2 \rightarrow Pt(PH_3)_2(H)_2$ and Important Geometric Parameters at the Transition State Obtained in Various ab Initio Studies

	$\Delta E_{act.}$, kcal/mol	R_{Pt-H}, Å	R_{H-H}, Å	Θ_{P-Pt-P}, deg
Noell and Hay[a]	17.4	1.81	0.90	120
Kitaura et al.[b]	5.2	2.066	0.766	147.7
this work	4.04	2.199	0.750	137.4

[a] Reference 30. [b] Reference 39.

The potential curves are shown in Figure 7, and the calculated energies are tabulated in Table V. The main effect of correlating the Pt–H bonds at the GVB–CI(2/6) level is to increase the exothermicity of the reaction and to move the transition state to longer distances. Correlating the nonbonding d electrons at the GVB–CI(2/6)*RCI(4/8) level makes the exothermicity for the reaction smaller than for the GVB–CI(2/6) level wave function, but gets essentially the same transition-state geometry and barrier. Correlating the nonbonding d electrons does not affect the long-range behavior of the Pt–H bonds. The GVB–CI(2/6) wave function (in which the nonbonding d electrons are doubly occupied) does as well as the GVB–CI(2/6)*RCI(4/8) wave function (which has the nonbonding d electrons correlated) near the transition state. This implies that this transition-state geometry is less sensitive to the s^1d^9–d^{10} splitting than is the exothermicity.

Qualitatively, these potential curves all have similar shapes. The potential curves for the correlated wave functions can be divided into three regions similar to those for the HF surface. This implies that the HF level wave function could have been used to elucidate the electronic structure of the mechanism. Unfortunately HF yields orbitals that are delocalized and difficult to interpret, whereas the GVB types of wave functions lead to orbitals that are localized and easier to interpret. Also, the GVB wave function allows one to interpret the various types of correlation and to see how each one affects the wave function. The GVB–CI(2/6) wave function leads to an improved description of the long-range attractive terms in the wave function, leading to a lower activation energy and a longer Pt–H bond distance at the transition state. At the GVB–CI(2/6)*RCI(4/8) level, we also include interpair correlations of the nonbonding d electrons on the platinum atom. These correlations were not important at the transition state because the Pt atom still has a d^{10}-like configuration. On the other hand, these d–d correlations have a big effect on the d^{10}–s^1d^9 separation, and hence they have a big effect on the reaction exothermicity. These correlation effects stabilize d^{10} relative to s^1d^9 and have led to a smaller exothermicity. In Table VI we present a summary of the energetics for oxidative addition at the different levels of calculation.

G. Comparison with Previous Results. The previous two ab initio studies of this system gave different results for activation barrier and transition state. A comparison of the results presented in this paper with the results from Noell and Hay and from Kitaura et al.[39] is shown in Table VII.

The transition-state geometry found in our studies and by Kitaura et al.[39] is much closer to products than Noell and Hay's[30] transition state. Also, our HF activation barrier (4.04 kcal) for oxidative addition is close to the value (5.2 kcal) found by Kitaura et al.[39] Noell and Hay,[30] on the other hand, found a significantly larger activation barrier (17.4 kcal/mol). Since we have used the same effective potential as Noell and Hay[37] and completely optimized the geometry for every fixed value of $Pt-H_2$ distance, Noell and Hay's[30] high activation barrier must be due to their partial optimization, which apparently did not converge to the lowest energy point along the reaction coordinate.

The differences between our transition-state geometry and that of Kitaura et al.[39] must be due to the different effective potentials and basis sets used. Our results should be more reliable for the following reasons. (1) We have used Noell and Hay's[37] Pt potential, which includes the f-projected terms required when f electrons are included in the effective potential, whereas the Kitaura et al.[39] calculations used an effective potential with only s and p projections. (2) We have used a larger hydrogen basis than Kitaura et al.[39] This larger basis includes the more diffuse character needed to describe the long-range $Pt-H_2$ interactions at the transition state.

The energies of reaction found from HF calculations in these three studies were also very different. Our ΔE (−16.2 kcal/mol) is larger than that found by Noell and Hay[30] (−6.7 kcal/mol), but smaller than the ΔE(−36.9 kcal/mol) of Kitaura et al.[39] We obtain a larger ΔE than Noell and Hay for this reaction because we allowed the Pt–P bond lengths to change along the reaction path. Noell and Hay held this parameter fixed at a value closer to the optimum for $Pt(PH_3)_2$, which should favor the dissociated limit and give a smaller ΔE. The Pt potential used by Kitaura et al.[39] is known to give Pt–H bonds that are 11.6 kcal/mol too strong.[30] Applying this correction factor to Kitaura et al.'s[39] ΔE leads to a corrected ΔE of 13.7 kcal/mol, which is very close to our value.

Comparing geometries with the available X-ray structures, we see that our Pt–P bond distances are too long by 0.1 to 0.2 Å. For $Pt(PCy_3)_2$, the experimental distance was found to be 2.231 Å,[5] while our calculated Pt–P bond distance for $Pt(PH_3)_2$ is 2.32 Å. Typical Pt–P bond distances for Pt(II) complexes are 2.25 Å for *t*-$H_2Pt(PCy_3)_2$,[40] 2.268 Å for *t*-$PtHCl[P(C_6H_5)C_2H_5]_2$,[41] and 2.248 Å for c-$PtCl_2(PMe_3)_2$.[42] Our calculated Pt–Pt bond distance for c-$H_2Pt(PH_3)_2$ is 2.45 Å, which is 0.2 Å too long. This elongation of the Pt–P bond length was also found by Noell and Hay[37] when they optimized the geometry of $Pt(PH_3)_2$ and found a Pt–P distance of 2.36 Å (using a different effective potential and basis set on the phosphorus). This effect appears to be systematic for phosphorus Lewis acid/Lewis base bonds treated at the HF level with a valence double-ζ basis.

In BH_3PH_3, where phosphorus is making a similar Lewis acid/Lewis base bond, we find a B–P bond length of 2.180 Å at the HF level using a double-ζ basis.[43] When the geometry was optimized with polarization functions on both the phosphorus and boron,[43] the B–P distance was found to be 2.055 Å. The experimental[44] B–P distance in BH_3PH_3 is 1.937 Å. Therefore, approximately 0.1 Å of the error observed in P Lewis acid/Lewis base bonds is due to the use of an unpolarized basis. Ahlrichs and Koch[45] have carried out calculations on BH_3PH_3 using a smaller basis set with both HF and correlated wave functions (CEPA). The smaller basis set yields a shorter B–P bond distance of 1.99 Å at the HF level. For the correlated wave function, their B–P bond distance is 0.04 Å shorter than their HF results. This indicates a large part of the remaining discrepancy must be due to electronic correlation.

Kitaura et al.[39] found Pt–P bonds that were short by 0.1 Å, but this is most likely due to the small basis set (STO-2G) used to optimize their geometries, which would underestimate bond distances for Lewis acid–Lewis base bonds.

(38) Noell, J. O. *Inorg. Chem.* **1982**, *21*, 11–14.
(39) Kitaura, K.; Obara, S.; Morokuma, K. *J. Am. Chem. Soc.* **1981**, *103*, 2891–2892.
(40) Immirzi, A.; Musco, A.; Carturan, G.; Belluco, U. *Inorg. Chim. Acta* **1975**, *12*, L13.
(41) Eisenberg, R.; Ibers, J. A. *Inorg. Chem.* **1965**, *4*, 473.
(42) Messmer, G. G.; Amma, E. L.; Ibers, J. A. *Inorg. Chem.* **1967**, *6*, 725.
(43) Dunning, T. H.; Hay, P. J. In "Modern Theoretical Chemistry: Methods of Electronic Structure Theory"; Schaefer, H. F., III, Ed.; Plenum Press: New York, 1977; Vol. 3, Chapter 1, pp 1–27.
(44) Durig, J. R.; Li, Y. S.; Carreira, L. A.; Odom, J. D. *J. Am. Chem. Soc.* **1973**, *95*, 2491–2496.
(45) Ahlrichs, R.; Koch, W. *Chem. Phys. Lett.* **1978**, *53*, 341–344.

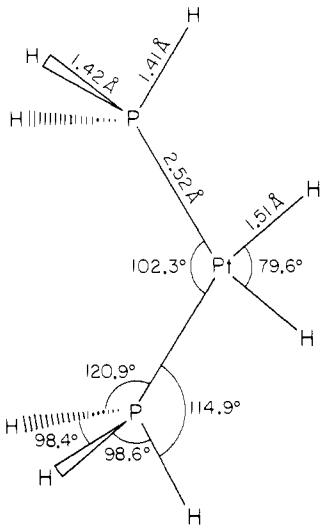

Figure 11. Geometry of $H_2Pt(PH_3)_2$ obtained by using a double-ζ basis on phosphines.

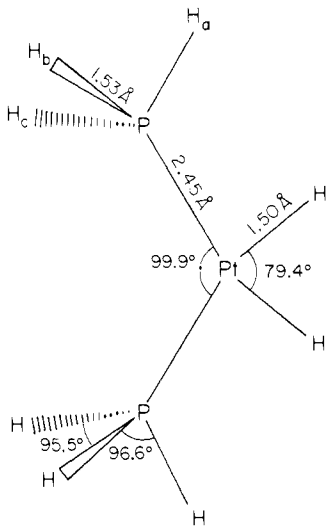

Figure 12. Geometry of $H_2Pt(PH_3)_2$ obtained by using a minimum basis on phosphines.

Hoffmann and co-workers[23] have performed an analysis of reductive elimination reactions using the extended Hückel method. Three major conclusions were presented in this work: (1) The better the σ-donating capability of the leaving group, the more readily the elimination proceeds. (2) Stronger donor ligands trans to the leaving groups give a higher barrier for the elimination reaction. (3) A lower positioning of the MA_2 b_2 orbital facilitates the reductive elimination of R_2. A lower MA_2 b_2 energy will be given by a lower metal d orbital energy.

Our studies concur with the third conclusion of Hoffmann et al. A more stable d orbital implies a more stable d^{10} state of the metal relative to s^1d^9 that will in turn increase the driving force for reductive elimination. This should also decrease the barrier for reductive elimination. Our results do not bear on the first two points since we have studied only the one system.

Balazs et al.[46] have also studied (1) using the SCF-Xα-SW approach. However, they do not report calculated geometries or transition states nor do they report calculated bond energies or activation energies; thus there is little with which to compare our work. The electronic densities from Xα agree with our results, indicating neutral H atoms (charge of −0.04 e).

IV. Calculational Details

A. Potentials and Basis Sets. On platinum atom we used the relativistic effective potential of Noell and Hay.[37] For the hydrogen atoms bonded directly to the Pt atom we used a triple-ζ contraction of Huzinaga's six-Gaussian basis.[47] For phosphorus we used the SHC effective potentials of Rappé et al.[48] with a minimum basis contraction based on the atomic orbitals. The hydrogen atoms bonded to P were described with a minimum basis set based on Huzinaga's four-Gaussian basis (unscaled). To determine whether the use of minimum basis phosphines affected the geometries or energetics for oxidative addition, we carried out geometry optimizations on $H_2Pt(PH_3)_2$ and $Pt(PH_3)_2$ using full double-ζ basis sets on the phosphine ligands. The results are shown in Figures 11 and 12. The exothermicity calculated for this reaction with double-ζ phosphines is 13.84 kcal/mol, only 2.47 kcal/mol smaller than the result with minimum basis set phosphines. This represents only a 1.25-kcal/mol error per Pt-H bond.

B. GVB-PP (Generalized Valence Bond with Perfect Pairing Restrictions).[49] In this wave function each correlated pair of electrons is described as a spin singlet state $\varphi_a\varphi_b + \varphi_b\varphi_a$. This description can be transformed to a natural orbital description

$$c_1\varphi_1^2 - c_2\varphi_2^2$$

where

$$\varphi_1 = \frac{(\varphi_a + \varphi_b)}{(2(1+S))^{1/2}} \qquad \varphi_2 = \frac{(\varphi_a - \varphi_b)}{(2(1-S))^{1/2}}$$

$c_2/c_1 = (1-S)/(1+S)$, $c_1^2 + c_2^2 = 1$, and $S = \langle\varphi_a|\varphi_b\rangle$. These natural orbitals are then used in higher level CI calculations.

C. GVB-RCI (Restricted Configuration Interaction). The GVB-RCI calculation includes the configurations φ_1^2, φ_2^2, and $\varphi_1\varphi_2$ for each GVB pair. When the configuration $\varphi_1\varphi_2$ is multiplied by similar configurations in the other GVB pairs, more general spin couplings are included that will optimize the total spin eigenfunction of the electronic wave function. This spin optimization can be important in describing the dissociation of multiple bonds and in describing the changes in the spin multiplicity in different atomic states. This wave function also includes interpair correlations important in the atomic d^{10}-s^1d^9 splittings. This type of wave function is useful because it still maintains orthogonal GVB pairs of electrons, facilitating the interpretation of the wave function.

When comparing singlet and triplet states of the platinum atom and of $Pt(PH_3)_2$, we counted the two open-shell orbitals as a GVB pair in the RCI(5/10) nomenclature. This is consistent since the triplet wave function contains all the configurations that the singlet contains except for those that have two electrons in one of the open-shell orbitals.

D. GVB-CI (Generalized Valence Bond Configuration Interaction). This type of CI is carried out by using all possible configurations that can be formed from the various occupations of the GVB orbitals from the GVB-PP calculation. This wave function includes all the terms of the RCI wave function plus terms that allow the GVB pairs to overlap and to change shape by allowing linear combinations between pairs. Such terms are particularly important near the region where the Pt-H bonds are just starting to form. Omission of such terms (as in a GVB-PP or RCI calculations) would lead to an artificial hump in the transition region.

Figure 13 demonstrates the importance of full correlation among the four electrons that are involved with the oxidation/reduction process. The GVB-PP wave function can describe the two Pt-H bonds at equilibrium or the doubly occupied d orbital and H-H bond at the dissociated limit. Near the region where both of the above VB descriptions are important, the energy of the GVB-PP wave function becomes artificially high. This gives a transition state near 1.55 Å for the GVB-PP wave function that disappears

(46) Balazs, A. C.; Johnson, K. H.; Whitesides, G. M. *Inorg. Chem.* **1982**, *21*, 2162–2174.
(47) Huzinaga, S. *J. Chem. Phys.* **1965**, *42*, 1293–1302.
(48) Rappé, A. K.; Smedley, T. A.; Goddard, W. A., III *J. Phys. Chem.* **1981**, *85*, 1662–1666.
(49) Bobrowicz, F. W.; Goddard, W. A., III In "Modern Theoretical Chemistry: Methods of Electronic Structure Theory"; Schaefer, H. F., III, Ed.; Plenum Press: New York, 1977; Vol. 3, Chapter 4, pp 79–127.

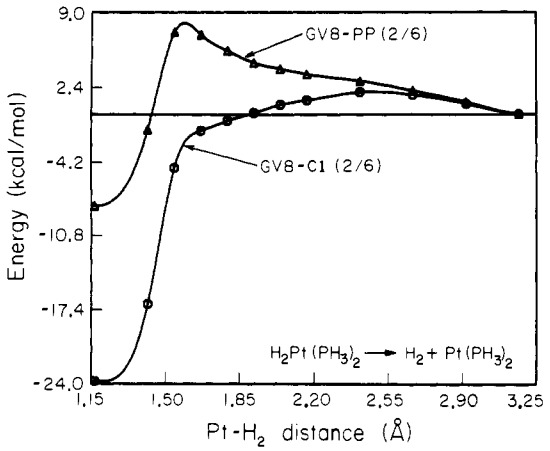

Figure Comparison of energies along the reaction coordinate for GVB-[illegible] 2/6) and GVB–CI(2/6) wave functions.

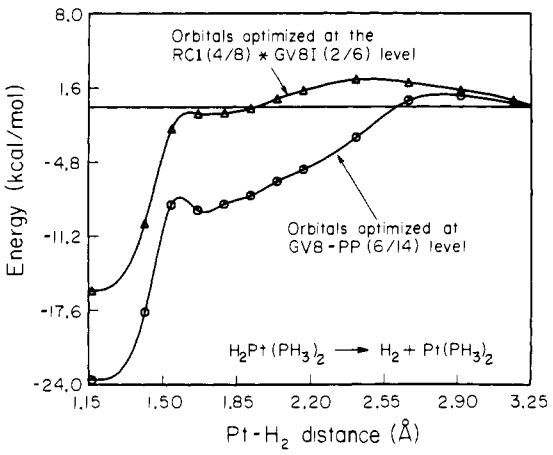

Figure 14. Comparison of energies along the reaction coordinate for RCI(4/8)*GVB–CI(2/6) and GVB–PP(6/14) wave functions.

for the GVB–CI wave function (which can describe both VB wave functions).

E. Geometry Optimizations. All of the geometry optimizations were obtained by using an analytic gradient procedure (GVBGRAD). This program was based on (a) the GVB2P5[49] program to evaluate density matrices for restricted HF and GVB–PP wave functions, (b) the HONDO[50] program to calculate derivatives of the ab initio terms in the energy expression, and (c) routines from the GAUSS 80[51] program and the Los Alamos effective potential program[52] to calculate the effective potential terms of the derivative. For the optimization of the geometries we used a relatively simple Newton–Raphson technique[36] in which the second derivative matrix is updated after every gradient calculation (except for the starting geometry).

The end-on approach of H_2 to $Pt(PH_3)_2$ was not considered in this work since the side-on approach of H_2 to $Pt(PH_3)$ gave a low barrier. The end-on approach should give a higher barrier because it would require breaking an H–H bond (104 kcal/mol) and promoting PtL_2 to a triplet state ($\sim$50 kcal/mol) while only getting $\sim$72 kcal/mol back in the Pt–H bond. [Kitaura et al.[39] found that the C_{2v} transition state is a true saddle point (i.e., there is only one negative root in the curvature matrix).]

F. Hybrid Wave Functions. In examining the effect of electronic correlation along the reaction path, we calculated a GVB–CI(2/6)*RCI(4/8) wave function where the orbitals were optimized for the full 3360 configuration (8568 spin eigenfunctions) wave function by using the GVB3[53] program. We used this wave function to examine the effects of correlating the nonbonding d electrons on the energetics along the reaction coordinate. The electrons in the Pt–H bonds were treated at the GVB–CI level for the reasons described above. The d nonbonding orbitals were treated at the RCI(4/8) level because this level was needed to get reasonable triplet–singlet splittings for the atom. The resulting wave function is therefore a product of the GVB(2/6) wave function for the Pt–H bonds and a RCI(4/8) for the nonbonding d electrons. This wave function was optimized self-consistently by using the GVB3 multiconfigurational self-consistent-field program[53] because the nonbonding d natural orbitals did not change smoothly from equilibrium to the dissociated limit at the GVB–PP level unless they were optimized at the CI level.

Often it is sufficient to use the orbitals from the GVB–PP wave function for RCI or GVB–CI wave functions. For example, orbitals obtained at the GVB–PP level were adequate for the GVB–CI(2/6) wave function. Optimizing the orbitals at the GVB–CI level lowered the energy of the GVB–CI wave function by less than 0.002 hartree (1.255 kcal/mol) relative to the GVB–CI calculation by using orbitals obtained at the GVB–PP level. This energy lowering remained essentially constant along the reaction path. Thus, although the GVB–PP wave function yields an unreasonable potential curve in the transition region, it does provide orbitals yielding a proper description of Pt–H bonding formation. This occurs because the GVB–CI includes the recoupling of bonding electrons necessary in describing the reaction.

However, for the GVB–CI(2/6)*RCI(4/8) wave function it is essential to self-consistently reoptimize the orbitals for the full wave function, as illustrated in Figure 14. The upper potential curve was obtained from the fully self-consistent wave function, while the lower curve is for a wave function for which the orbitals were optimized at the GVB–PP level. Use of incompletely optimized orbitals (GVB–PP) is biased against the Pt d^{10} state (the dissociated limit) and leads to an irregularly stepped potential curve. The reason for this behavior is that for $Pt(PH_3)_2$ the RCI wave function includes terms differential in the d^{10}–s^1d^9 splitting. When the orbitals are optimized for a wave function including these terms, orbital shape changes occur that are differential for these state splittings. These differential terms affect the shape of the potential curve (and the transition state) because the platinum atom changes its electronic state during the reaction.

Acknowledgment. This work was supported in part by a grant from the National Science Foundation (No. CHE80-17774). One of the authors (J.J.L.) wishes to acknowledge financial support in the form of a fellowship from Exxon.

Registry No. $Pt(H)_2(PH_3)_2$, 76832-29-6; $Pt(PH_3)_2$, 76830-85-8; H_2, 1333-74-0.

(50) Dupuis, M.; King, H. F. *J. Chem. Phys.* **1978**, *68*, 3998–4004.
(51) Binkley, J. S.; Whiteside, R. A.; Krishnan, R.; Seeger, R.; DeFrees, D. J.; Schlegel, H. B.; Topiol. S. W.; Kahn, L. R.; Pople, J. A. "Gauss 80", unpublished.
(52) Hay, P. J.; Wadt, W. R.; Kahn, L. R., unpublished results.
(53) Yaffe, L. G.; Goddard, W. A., III *Phys Rev. A* **1976**, *13*, 1682.